Geochemistry of Nevado de Longaví Volcano (36.2°S): a compositionally atypical arc volcano in the Southern Volcanic Zone of the Andes

Selles, Daniel; Rodriguez Soto, Ana Carolina; Dungan, Michael; Naranjo, José A.; Gardeweg, Moyra

How to cite

SELLES, Daniel et al. Geochemistry of Nevado de Longaví Volcano (36.2°S): a compositionally atypical arc volcano in the Southern Volcanic Zone of the Andes. In: Revista geológica de Chile, 2004, vol. 31, n° 2, p. 293–315. doi: 10.5027/andgeoV31n2-a08

This publication URL: https://archive-ouverte.unige.ch/unige:154587
Publication DOI: 10.5027/andgeoV31n2-a08

Geochemistry of Nevado de Longaví Volcano (36.2°S): a compositionally atypical arc volcano in the Southern Volcanic Zone of the Andes

Daniel Sellés
A. Carolina Rodríguez
Michael A. Dungan

Section de Sciences de la Terre, University of Geneva
13 Rue des Maraîchers, 1205 Geneva, Switzerland
daniel.selles@terre.unige.ch
carolina.rodriguez@terre.unige.ch
michael.dungan@terre.unige.ch

José A. Naranjo

Servicio Nacional de Geología y Minería, Chile
jnaranjo@sernageomin.cl

Moyra Gardeweg

Aurum Consultores, Santiago, Chile
mgardeweg@manquehue.net

ABSTRACT

The Quaternary Nevado de Longaví volcano of the Andean Southern Volcanic Zone (SVZ) has erupted magmas that range in composition from basalt to low-silica dacite, although andesites are the dominant erupted magma type. Amphibole is a common phenocryst phase in andesites throughout the volcano, and it is the dominant mafic phase in Holocene dacites and their included mafic enclaves. Compositions of magmas erupted at Longaví volcano define arrays that diverge from trends delineated by neighboring frontal-arc volcanoes. Although mafic compositions at Longaví are broadly similar to basalts at other SVZ centers, Longaví intermediate and evolved magmas have systematically lower abundances of incompatible major (K_2O, P_2O_5) and trace elements (Rb, Zr, Nb, REE, Th, etc), as well as high Ba/Th, Sr/Y, and La/Yb ratios. Longaví volcano magmas define two differentiation series with regard to enrichments of Rb (and other incompatible elements) with increasing silica. A high-Rb series that includes the oldest units of the volcano comprises basalts to andesites dominated by anhydrous mineral assemblages with chemical compositions similar to other SVZ magmatic series. The series with low Rb, on the other hand, includes the Holocene units that evolved from basaltic andesites to dacites by means of fractional crystallization wherein amphibole and calcic plagioclase dominate the mineral assemblage. Magmas parental to low-Rb series are interpreted to be high-degree mantle melts, highly hydrous and oxidized, formed as a response to high fluid inputs into the subarc mantle. Enhanced water transport to the subarc mantle is a plausible effect of the subduction of the oceanic Mocha Fracture Zone that projects beneath Nevado de Longaví. Volcanoes located over oceanic fracture zones further south along the SVZ have erupted hornblende-bearing magmas that share some chemical similarities with Longaví volcano magmas.

Key words: Southern Volcanic Zone, Nevado de Longaví volcano, SVZ segmentation, Amphibole fractionation.

RESUMEN

Geoquímica del volcán Nevado de Longaví (36,2°S): un volcán de arco composicionalmente atípico en la Zona Volcánica Sur de los Andes. El estratovolcán cuaternario Nevado de Longaví de la Zona Volcánica Sur de los Andes (ZVS) ha emitido magmas de composición basáltica a dacítica, si bien los productos predominantes son andesíticos. La anfíbola es fenocristal común en andesitas de todo el volcán, y es la fase máfica predominante en dacitas de edad holocena y en enclaves máficos coetáneos. La composición química de los magmas del Nevado de Longaví define patrones que difieren de las tendencias mostradas por otros centros del frente volcánico. Si bien las lavas máficas del Nevado de Longaví son, en términos generales, similares a otros basaltos de la ZVS, las lavas intermedias y evolucionadas exhiben valores sistemáticamente bajos de elementos incompatibles, tanto mayores (K_2O, P_2O_5) como trazas (Rb, Zr, Nb, REE, Th, etc), así como altos valores de Ba/Th, Sr/Y y La/Yb. Dos series magmáticas se definen en base al grado de enriquecimiento en Rb (y otros elementos incompatibles) con el aumento de sílice. La serie de alto Rb, que incluye a las unidades más antiguas del volcán, pero que podría ser en parte coetánea a la serie de bajo Rb, está conformada por basaltos a andesitas de composición química próxima a otras series magmáticas de la ZVS dominadas por asociaciones minerales anhidras. La serie de bajo Rb, que incluye a las unidades holocenas del volcán, evoluciona desde andesitas basálticas a dacitas por vía de cristalización fraccionada involucrando importantes proporciones de anfíbola y plagioclasa cálcica. Los magmas parentales de esta serie serían fundidos parciales de alto grado, altamente hidratados y oxidados, consecuencia de un elevado aporte de agua a la fuente astenosférica. Un elevado transporte de agua hacia el manto astenosférico probablemente resulta de la subducción de la Zona de Fractura oceánica Mocha que se proyecta bajo el Nevado de Longaví. Otros volcanes de la ZVS situados sobre fracturas oceánicas han emitido magmas con anfíbola que comparten algunas similitudes químicas con los magmas del Nevado de Longaví.

Palabras clave: Zona Volcanica Sur, Volcán Nevado de Longaví, Segmentación de la ZVS, Fraccionamiento de anfíbola.

INTRODUCTION

First-order geodynamic factors that may control arc magma chemistry include: 1) subducting plate parameters such as thermal state and buoyancy of the slab, depth and extent of dehydration, ability to drag trench sediments and/or to erode the forearc lithosphere; 2) the chemistry and mineralogy of the sub-arc asthenospheric mantle, as well as melting and melt migration mechanisms involved in basalt generation, and 3) the potential of the overriding plate to contaminate mantle-derived magmas, which can be a function of crustal thickness, lithologic composition, and stress regime. The mutual interdependence of some of these factors (*e.g.,* length and depth of melting of the mantle column will vary with thickness of the overriding plate; stress regime of the continental plate can be related to buoyancy of the subducted plate) further complicates the quantification of the conditions that control magma evolution paths in the course of the construction of large volcanic edifices.

The Southern Volcanic Zone of the Andes (SVZ) is an example of a volcanic arc that exhibits systematic along-strike chemical and mineralogical variations which have been related to regional-scale variations in some of these factors. We present whole-rock and mineral chemistry data from lavas of the Nevado de Longaví volcano that do not conform to previously documented along-arc chemical variations, and which challenge existing composition-based schemes for division of the arc into magmatic provinces. Although most of the broad-scale variations within the SVZ lend themselves to explanations linked to upper-plate controls, namely crustal thickness and age, the unusual chemistry and mineralogy of Nevado de Longaví magmas may be best explained by the local character of the oceanic plate.

Holocene hornblende-bearing dacites erupted at Longaví volcano show geochemical and mineralogical characteristics that render them different from other dacites of the SVZ. Low abundances of incompatible elements coupled with high Sr/Y and LREE/HREE ratios, and relatively high Mg and Cr contents are among the characteristics that distinguish Longaví dacites from evolved magmas elsewhere in the SVZ. Longaví dacites have an 'adakitic' chemical signature (without implying any particular genesis). The presence of presumably cogenetic mafic magmas allows the evolution of Longaví dacites to be tested. We present the first overview of the magmatic evolution of Nevado de Longaví based on the volcanic stratigraphy, whole-rock major and trace element chemistry, petrography, and mineral chemistry, and present a working hypothesis for the formation of these magmas.

GENERAL SVZ FRAMEWORK

The SVZ is the Quaternary volcanic arc developed on the western margin of the South American plate that extends between latitudes 33 and 46°S (Fig. 1 and Stern, 2004). The SVZ is separated from the Central and Austral Volcanic Zones by volcanic gaps that coincide with the subduction of the aseismic Juan Fernández Ridge and the active Chile Rise respectively. Between these latitudes, the estimated thickness of the continental crust varies from ~55-65 km in the north to ~30-35 km in the south (Hildreth and Moorbath, 1988), and frontal-arc volcanoes are located at progressively lower altitudes, ranging from 4500 m in the north to sea-level in the south. The chemistry and mineralogy of the arc's eruptive products vary with latitude. Volcanic centers close to the northern termination of the SVZ (33-34.5°S) are composed primarily of andesites and more evolved lavas wherein hydrous mineral phases are common and olivine is usually absent. These variably evolved lavas are characterized by the highest contents of incompatible elements (for a given SiO_2 content) within the SVZ. In contrast, volcanoes from 37 to 41.2°S are largely composed of mafic lavas and they occur west of the continental divide, located progressively closer to the Central Depression and at lower base elevations to the south. Evolved magmas rarely contain hydrous minerals and are

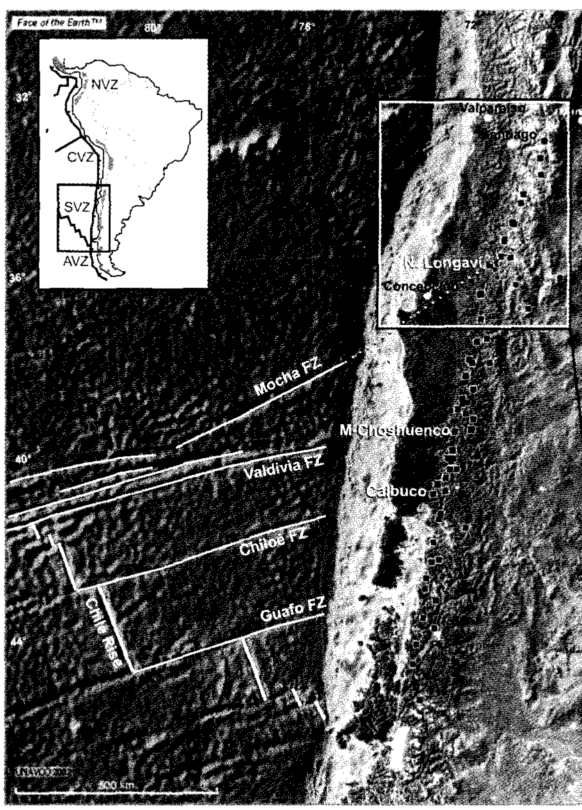

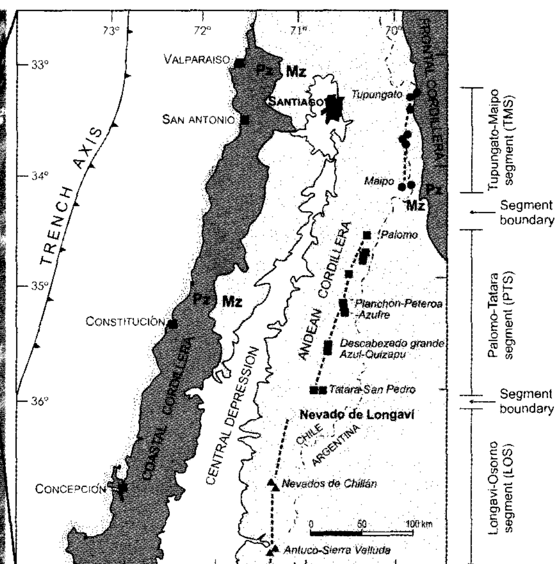

FIG. 1. Location of Nevado de Longaví volcano and some other volcanic centers of the SVZ. Digital elevation model is reproduced from http://jules.unavco.ucar.edu (Face of the Earth is a registered trademark, ARC Science Simulations © 1999). Inset to the left shows the position of the SVZ relative to the Northern, Central and Austral volcanic zones (NVZ, CVZ, and AVZ respectively). The location of oceanic fracture zones and the Chile Rise are annotated in white (after Tebbens and Cande, 1997; Herron, 1981). Panel to right zooms to the northern end of the SVZ and shows the segmentation scheme used in text; figure modified from Hildreth and Moorbath (1988) after Wood and Nelson (1988) and Dungan *et al.* (2001). The oldest age of exposed basement units is indicated as Paleozoic (Pz) or Mesozoic (Mz). Segmented line indicates the location of the volcanic front.

less enriched in incompatible elements than are lavas to the north. A much greater extent of crustal contamination is also inferred in northern volcanoes on the basis of isotopic signatures. Volcanoes located between these two extremes occur at progressively higher base elevations to the north, and they are intermediate in terms of some geochemical parameters such as Sr isotopic ratios (Fig. 2).

Although arc-scale systematic variations in magma composition have been recognized previously in the SVZ, there is little consensus on the origin of these geographic trends. The relative roles of depth of magma differentiation, the proportion and chemical signature of continental crust assimilated during magma storage and ascent, source contributions related to sediment subduction and tectonic erosion, and the length of the asthenospheric melting column are currently a matter of debate (Hildreth and Moorbath, 1988; Futa and Stern, 1988; Sigmarsson *et al.*, 1990; Stern, 1991; Hildreth and Moorbath, 1991; Tormey *et al.*, 1991).

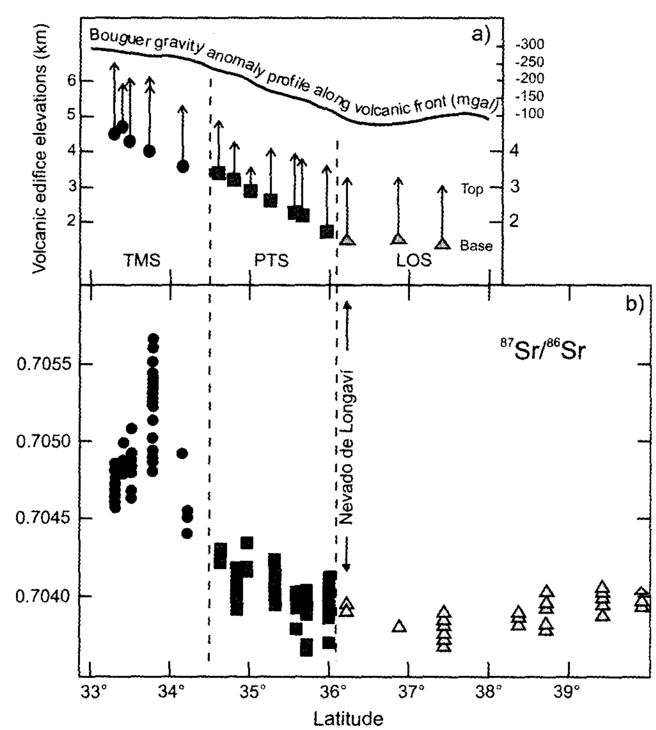

FIG. 2. **a.** Basal and summit elevations of centers along the volcanic front between 33 and 37.5°S relative to sea level. These topographic data and the Bouguer gravity-anomaly profile along the arc suggest increasing crustal thickness to the north of Longaví; **b.** Sr isotopic ratios *versus* latitude for volcanic front centers. Both figures are taken from Hildreth and Moorbath (1988) where original data sources are cited. TMS, PTS, and LOS refer to segments shown in figure 1.

A number of different schemes have been proposed for grouping SVZ volcanoes into provinces or segments. The location of boundaries, nomenclature, and the criteria for defining these subdivisions vary from one scheme to the next (Fig. 3). The authors have adopted the segmentation nomenclature proposed by Dungan *et al.* (2001), based on arguments by Wood and Nelson (1988), wherein the arc has been divided according to changes in orientation and lateral shifts in the position of the volcanic front, and segments are named after the northernmost and southernmost volcanic center in each segment.

The northernmost SVZ or Tupungato-Maipo Segment (TMS; Fig. 1) of Dungan *et al.* (2001) comprises the north-south trending Quaternary volcanic centers located at the crest of the Andean range between 33 and 34.5°S. Magmas erupted in

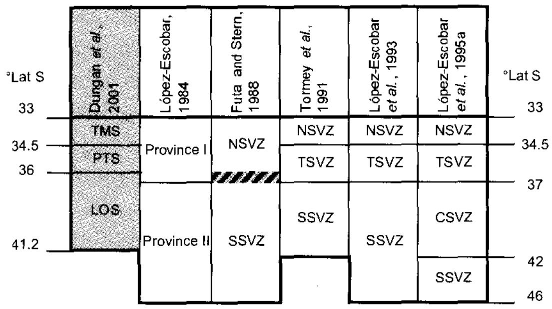

FIG. 3. Comparison of the SVZ segmentation scheme used in this article (first column, after Dungan *et al.*, 2001) to other schemes. Note that the main difference is related to the placement of a segment boundary at 36 *versus* 37°S. NSVZ, TSVZ, CSVZ, and SSVZ stand for northern, transitional, central, and southern SVZ respectively. TMS, PTS and LOS are acronyms for Tupungato-Maipo, Palomo-Tatara, and Longaví-Osorno Segments respectively.

this segment are dominantly andesitic or more evolved, and mafic magmas (<54% SiO_2) have not been observed. High abundances of incompatible elements, coupled with high Sr isotopic ratios in volcanic rocks from this segment are considered to be a consequence of substantial amounts of lower crustal assimilation by mantle derived magmas (Hildreth and Moorbath, 1988; Ruiz *et al.*, 2001). Alternatively, they may also be the result of source contamination by subduction of trench sediments and/or erosion and drag of forearc lower crust (Futa and Stern, 1988; Stern, 1991). South of this segment, the Palomo-Tatara Segment (PTS; 34.5-36°S) trends slightly oblique to the Andean crest and the volcanoes are located at progressively lower altitudes to the south. Andesites are the most abundant products, although the proportions of basaltic andesites and basalts increase southward, and are dominant at Planchón volcano (35.2°S; Naranjo and Haller, 2002) and in the Tatara-San Pedro complex (36°S). Crustal contributions to evolved magmas are well documented within the Planchón-Peteroa (Tormey *et al.*, 1995) and Tatara-San Pedro (Davidson *et al.*, 1987) complexes. South of 36°S extends the central SVZ or Longaví-Osorno Segment (LOS, 36-41.2°S), wherein the trend of frontal-arc volcanoes is nearly parallel to the cordilleran axis, and the basal elevation of centers varies less steeply. Volcanic edifices within this segment are mostly dominated by mafic lavas.

Previous composition-based subdivisions considered Nevado de Longaví and Nevados de Chillán volcanoes, both dominantly andesitic, to be part of the 'transitional' SVZ. Tormey *et al.* (1991) suggest that 37°S (*i.e.*, south of Nevados de Chillán) is the point where: 1) the thickness of the crust below the volcanic front starts to sharply increase northwards, and 2) the axis of the arc intersects the subsurface projection of the oceanic Mocha Fracture Zone. Both of theses inferences, however, seem to be incorrect. Figure 2 shows that along the volcanic front, basal elevations of volcanoes and Bouguer gravity anomalies have inflection points around 36°S. Likewise, when the projection of the Mocha Fracture Zone is corrected for the dip of the slab (30°; Bohm *et al.*, 2002), it intersects the arc close to Nevado de Longaví rather than south of Nevados de Chillán. A segment boundary at 36°S leaves the andesitic Longaví and Chillán edifices grouped together with more mafic volcanoes to the south, but unlike andesitic volcanoes north of 36°S, evolved lavas from Longaví and Chillán do not seem to have experienced significant crustal contamination (not more than volcanoes to the south, in any case), or at least the chemical signature of contamination is much less 'enriched' than it is to the north. Calbuco volcano (42°S) is in many ways different from volcanoes to the north (much like Longaví volcano, López-Escobar *et al.*, 1995b).

NEVADO DE LONGAVÍ VOLCANO

Nevado de Longaví is a late Quaternary SVZ stratovolcano located at 36°12'S-71°10'W (Fig. 1). Reconnaissance mapping by Gardeweg (1980 and 1981) was included within the regional framework presented by Muñoz and Niemeyer (1984), and analyses of various samples from Longaví volcano were discussed by Hildreth and Moorbath (1988) and Hickey *et al.* (1984). The volcanic edifice was constructed on folded volcaniclastic strata of the Cura-Mallín Formation (Eocene to Early Miocene; Muñoz and Niemeyer, 1984), which is intruded by Miocene plutons, and uncomformably covered by basaltic to basaltic andesitic lavas and breccias of the Late Pliocene-Pleistocene Cola de Zorro Formation. South of Longaví volcano, in the Cordón de Villalobos, outcrops of this formation define a large, low-profile, deeply eroded volcanic edifice. Nevado de Longaví volcano is a relatively small, single cone (basal altitude ~1,500 m; summit altitude 3242 m; ~20 km^3 estimated volume), mainly composed of thick andesitic flows that radiate from the current summit area. There is no evidence of caldera-forming eruptions but sector collapse scars are present on the east and southwestern slopes of the cone (Fig. 4). No historical eruptions are recorded, although Holocene volcanism was frequently explosive and the pyroclastic deposits from this phase of activity partly fill the sector-collapse depression on the east flank (headwaters of Río Blanco).

Lavas from Longaví volcano range in composition from basalts to dacites (51-65 wt% SiO_2). Andesites with 56-60 wt% SiO_2 are the most abundant products and represent more than 80% of the total output. Basaltic (51.5 wt% SiO_2) and dacitic (64-65 wt% SiO_2) products are subordinate. Dacitic compositions have been only identified among Holocene units, and scarce basalts are found within the mainly basaltic andesitic early stages of growth of the edifice. Fine-grained magmatic enclaves of basaltic andesitic composition are common, and locally very abundant in andesitic and dacitic lavas.

EARLY UNITS

The oldest units of Longaví volcano are sequences of basaltic andesitic flows that are exposed on the north and southwest flank of the edifice (Fig. 4). The northern flank of the volcano exposes a 100-150 m thick sequence of basaltic and basaltic andesitic flows (51.9 to 54.3 wt% SiO_2) that radiate from a point ~400 m lower than the present-day summit. This inferred fossil vent is now occupied by a partly intrusive andesitic dome. Individual lava flows are 1-3 m thick, but massive flows pinch out towards the vent where mafic scoriaceous deposits form up to 80% of the exposures, probably reflecting dominantly strombolian eruption style. Abundant plagioclase (plag, An_{60-75}) +olivine (oliv, Fo_{70-75}) +clinopyroxene (cpx, $En_{43-45}Wo_{39-43}Fs_{13-14}$) phenocrysts in an intergranular groundmass are characteristic of this unit. A sequence of basaltic andesites with similar composition and mineralogy is exposed on the south wall of Quebrada Los Bueyes (Fig. 4). The total exposed thickness is about 150 m, the base of which corresponds to ~50 m of mafic epiclastic and pyroclastic beds that directly overlie basement-derived colluvium and *in situ* Cura-Mallín basement. The upper part of the sequence is composed of olivine-phyric basaltic andesitic flows, 1-5 m thick each, which are in turn covered by thicker, amphibole-bearing andesites.

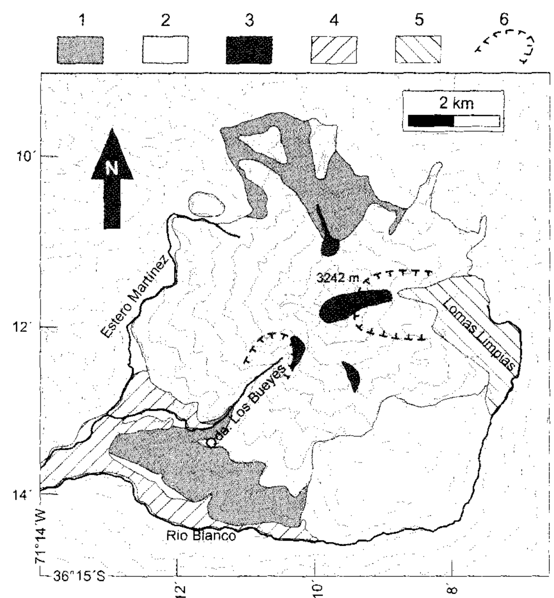

FIG. 4. Schematic map of Nevado de Longaví volcano showing the units discussed in the text. **1.** Early units, mainly basaltic andesitic lava flows. **2.** Main cone andesites. **3.** Summit area andesitic to dacitic domes, central dome of presumably Holocene age. **4.** Pre-Holocene terrace deposits associated to Los Bueyes sector collapse and Martínez and Río Blanco streams. **5.** Holocene pyroclastic deposits of Lomas Limpias collapse bowl. **6.** Collapse scars. Contour curves every 200 m.

CONE-FORMING UNITS

The main cone of Nevado de Longaví volcano is composed of thick (4-15 m) lava flows and flow breccias that radiate from the summit area. Lavas forming the main cone are andesites with 55.1-62.2 wt% SiO_2 (most of them between 57 and 61%, though), wherein the typical mineral association is plag+opx (En_{65-76})+cpx ($En_{35-50}Wo_{37-48}Fs_{8-15}$)±oliv ($Fo_{70-81}$)±amph. Both olivine and amphibole commonly show disequilibrium reaction textures, especially when they coexist in the same host. Lava flows also commonly contain abundant amphibole-bearing gabbroic fragments and quenched mafic enclaves (see below). Internal stratigraphy is difficult to extend from one locality to another due to the homogeneous compositions involved and because the source area seems to have remained static throughout the construction of the edifice. Important erosion periods, however, are recorded within the units on the northern flank of the volcano, where late lavas, themselves glaciated, have flowed into deep U-shaped valleys excavated into older andesites.

HOLOCENE UNITS

Holocene activity was concentrated in the summit area and on the eastern flank of the edifice, which has been substantially modified by pre-Holocene flank failure and collapse. The Lomas Limpias sector collapse depression (~2 km^2; Fig. 5) was subsequently partially filled with effusive and pyroclastic materials of Holocene age that range in composition from basaltic andesitic to dacitic, and therefore span a broader compositional range than the main edifice.

The oldest deposits (unknown age) exposed in the collapse depression comprise a thin (~30m) volcaniclastic sequence formed by an alternation of decimeter thick, coarsely reverse-graded breccias with sandy matrices and centimeter-thick beds of fine sand and silt. The breccias host fragments of glassy basaltic andesites and andesites up to 20 cm in diameter, which are variably vesiculated and contain plag +oliv +cpx phenocrysts. These clastic beds interfinger with thin basaltic flows and hyaloclastic breccias that have the same composition as the associated clasts, which range from 52 to 62% SiO_2, and which have the highest K_2O contents found at Longaví volcano. These deposits, which may have been erupted sub-glacially, are overlain by a more silicic sequence of pyroclastic and effusive units in which three distinct evolved magma compositions are present.

The first of these is a thick, white pumice fall deposit that proximally overlies the volcaniclastic deposits and that extends for more than 20 km to the southeast of Longaví volcano. Proximal pumice accumulations have a maximum thickness of 30 m, although the deposits thin rapidly away from the summit and in the collapse bowl pumice accumulation is <15 m thick. The pumices have a dacitic composition (65.1-65.8 wt% SiO_2) and host amph +plag ±opx phenocrysts. Charcoal collected from below the pumice deposit has yielded a ^{14}C age of 6,835±65 ybp[1].

The second is a thick andesitic lava flow (59.8 wt% SiO_2) that postdates the pumice bed. It is confined to the proximal collapse bowl and partially fills an erosional depression cut into the white pumice. The phenocryst assemblage of this less evolved magma includes olivine (Fo_{79-80}) and orthopyroxene (En_{70-74}) phenocrysts in addition to plagioclase and oxidized amphibole. Abundant fine-grained and plutonic- and cumulate-textured enclaves are present.

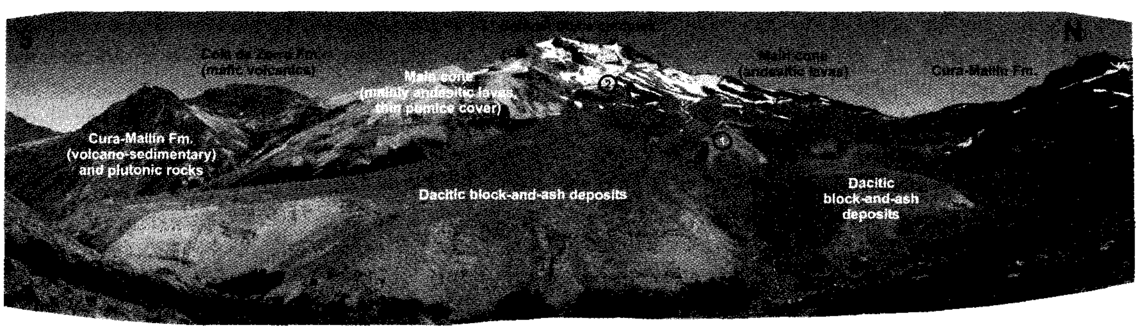

FIG. 5. Panoramic view of the eastern flank of Nevado de Longaví volcano, showing the Lomas Limpias collapse bowl and deposits filling the depression. In the foreground, dacitic block and ash deposits from collapse of summit dome overlying hyaloclastic breccias (1) and Holocene andesitic lava (2). Main cone andesites are partly covered by ~7000 ybp pumice fall deposit. Left (south) of the volcano crop out Cura-Mallín Formation volcaniclastic strata intruded by Miocene granitoids and covered by Plio-Pleistocene mafic lavas from the Villalobos volcano (Cola de Zorro Formation).

1 Necessary preparation and pre-treatment of the sample material for radiocarbon dating was carried out by the ^{14}C laboratory of the Department of Geography at the University of Zurich (GIUZ). The dating itself was done by AMS (accelerator mass spectrometry) with the tandem accelerator of the Institute of Particle Physics at the Swiss Federal Institute of Technology Zurich (ETZ). This age is part of C. Rodríguez's Ph.D. research project.

The last volcanic event recorded at the volcano is the extrusion of a dacitic (63.1-64.3 wt% SiO_2) dome in the upper part of the collapse bowl and part of the summit area. The dome partly collapsed towards the east, forming block and ash deposits (estimated volume ~0.12 km^3) that cover most of the previously described deposits. These dacitic magmas contain abundant calcic amphibole phenocrysts, as well as zoned plagioclase (An_{60-30}) and lesser amounts of orthopyroxene ($En_{\sim70}$). The dacite also contains a high proportion (~3%) of quenched mafic enclaves. The major and trace element composition of this dacite is similar to that of the underlying pumices and they constitute the most evolved products found at Longaví volcano. Other amphibole-bearing andesitic domes have been found intercalated in lava flows around the summit area, but their age is unknown.

PLUTONIC-TEXTURED AND QUENCHED MAFIC ENCLAVES

Lavas from Nevado de Longaví volcano commonly contain abundant fine-grained inclusions and coarse- to medium-grained plutonic-textured fragments. The authors refer to them as 'fine-grained' or 'quenched' enclaves if they display textures indicative of injection in a molten state and for which whole-rock chemistry can be considered to represent the composition of a magma. 'Plutonic-textured' or 'coarse-grained' enclaves are fragments that were mostly crystalline when incorporated into the host magma, and that do not necessarily correspond to a magma composition (*e.g.,* cumulates).

Quenched mafic enclaves are gray to dark green, fine-grained, crystal-rich (<15% interstitial glass), rounded, and up to 40 cm in diameter. Acicular microphenocrysts of amphibole and plagioclase are set in a vesiculated glassy groundmass that contains smaller clinopyroxene and iron-oxide granules. Plagioclase, pyroxene, and olivine phenocrysts (variably reacted or overgrown) are rare. Whole-rock compositions of quenched enclaves range from 52 to 59 wt% SiO_2, although quenched enclaves in the Holocene dacites are slightly richer in silica (53.8-58.8%) than fine-grained enclaves from the rest of the volcano (52.3-56.5%). Partially resorbed plagioclase xenocrysts incorporated into quenched enclaves from the host dacite record mixing (Feeley and Dungan, 1996), which causes them to depart to varying degrees from the original liquid composition.

Plutonic textured enclaves are of two main types: 1. Biotite and quartz-bearing granitoids, and 2. Hornblende-rich gabbroids. Granitoid xenoliths have only been found in the Holocene pumice-fall deposit as accidental ballistic fragments. They are petrologically and chemically similar to Miocene plutons that crop out in this area, and lack evidence of partial melting or other reactions with the juvenile magma despite their fertile mineralogy. Thus, as they probably were ripped from the basement at shallow levels during the explosive eruption and have not participated as contaminants of the magmatic system, they are not considered further.

Gabbroic plutonic-textured enclaves (44-56% SiO_2) are common in the cone-forming and Holocene units, and are very abundant in certain flows (~5% volume). Plutonic-textured enclaves are rounded or occasionally angular, ranging from less than a centimeter to >30 cm in diameter. They are primarily medium- to coarse-grained hornblende gabbros and pyroxene-hornblende norites and gabbronorites (nomenclature after Le Maitre, 1989). Gabbroic enclaves are composed of calcic amphibole (pargasite, magnesio-hastingsite), calcic plagioclase (An_{80-90}), less abundant orthopyroxene (En_{71-80}), and scarce clinopyroxene ($En_{43-45}Wo_{45-47}Fs_{10-11}$); olivine ($Fo_{76-89}$) is present as rounded cores in some amphiboles. Amphibole is mantled by dehydration coronas that range from opaque margins with irregular interior limits to fine-grained aggregates of clino- and orthopyroxene plus less calcic plagioclase ($An_{\sim40-65}$) and iron oxides. These textures are probably due to dehydration reactions and are often associated with grain-boundary partial melting that can represent up to 30% volume in some samples. The grain boundary melts crystallized to plagioclase and pyroxene microlites (±apatite) upon eruption. The most mafic of the coarse-grained enclaves, which display cumulate textures (Fig. 6a), are composed of up to 70% amphibole, less than 20% plagioclase and 10% of a probably residual interstitial liquid. Large crystals of interstitial plagioclase commonly contain small amphibole inclusions indicating that amphibole and plagioclase could have co-crystallized. The authors will show below that the compositions of these amphiboles are indistinguishable within error from those found in Longaví lavas, which suggests that gabbroic enclaves represent cumulates related to the active magmatic system, not fragments of unrelated crust.

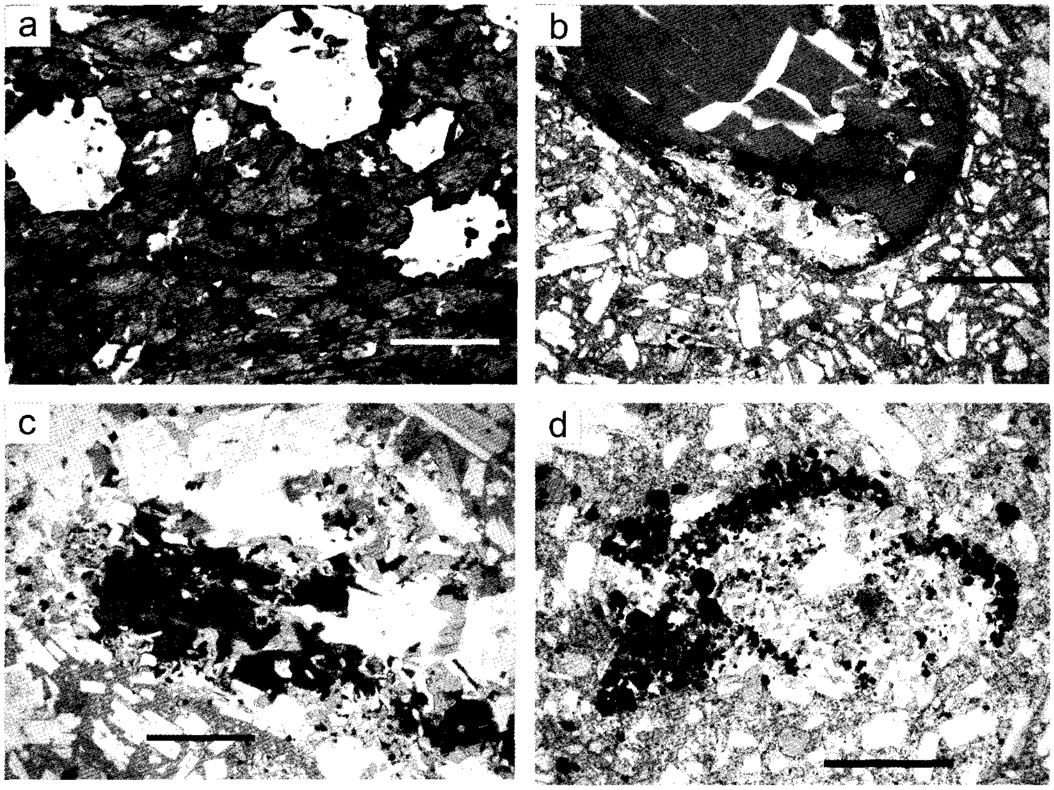

FIG. 6. **a.** Cumulate texture in a gabbroic enclave (NL 120E). Note alignment of dark amphibole crystals and small amphibole inclusions within plagioclase (clear). Amphibole phenocrysts in Longaví magmas are replaced to varying extents by reaction products; **b.** Fine-grained dusty magnetite amphibole breakdown zone localized along the grain margin; **c.** More advanced reaction involving extensive replacement of the grain interior; **d.** Complete replacement of an amphibole grain wherein the original outline of the amphibole is marked by concentrations of oxides. Scale bars = 1 mm.

WHOLE ROCK CHEMISTRY AND COMPARISON WITH THE SVZ

Nevado de Longaví mafic magmas overlap extensively for major and trace elements with basaltic rocks from both the LOS (Longaví-Osorno Segment) and PTS (Palomo-Tatara Segment; Fig. 3). However, for rocks with SiO_2 >56 wt% they display chemical variation trends that are in many ways dissimilar to SVZ volcanoes located to the north and to the south (Fig. 7). We stress that Longaví volcano, which lies at the segment boundary in an intermediate geographic position, does not define trends that are intermediate between typical LOS and PTS lavas, and that this distinction becomes increasingly well defined with increasing SiO_2. Longaví magmas are characterized by: 1) high Al_2O_3, CaO, and Sr contents (Fig. 7a-b-c) that lie at the upper limits of both the PTS and LOS data for magmas with >56 wt% SiO_2, 2) correspondingly low TiO_2 and Fe_2O_3 contents (Fig. 7d) in mafic and intermediate compositions, 3) moderately high MgO and Cr contents (Fig. 7e-f) in intermediate and evolved compositions, and 4) low concentrations of a variety of incompatible element, including P_2O_5, K_2O, LILE, HFSE and REE (Fig. 7g-h-i-j) which are most pronounced in intermediate and evolved compositions. In summary, elements that are most compatible with plagioclase and olivine plus Cr-spinel have the highest relative concentrations, whereas elements such as K, which would increase most rapidly in the case of crustal assimilation, are low in Longaví andesites relative to all other SVZ centers.

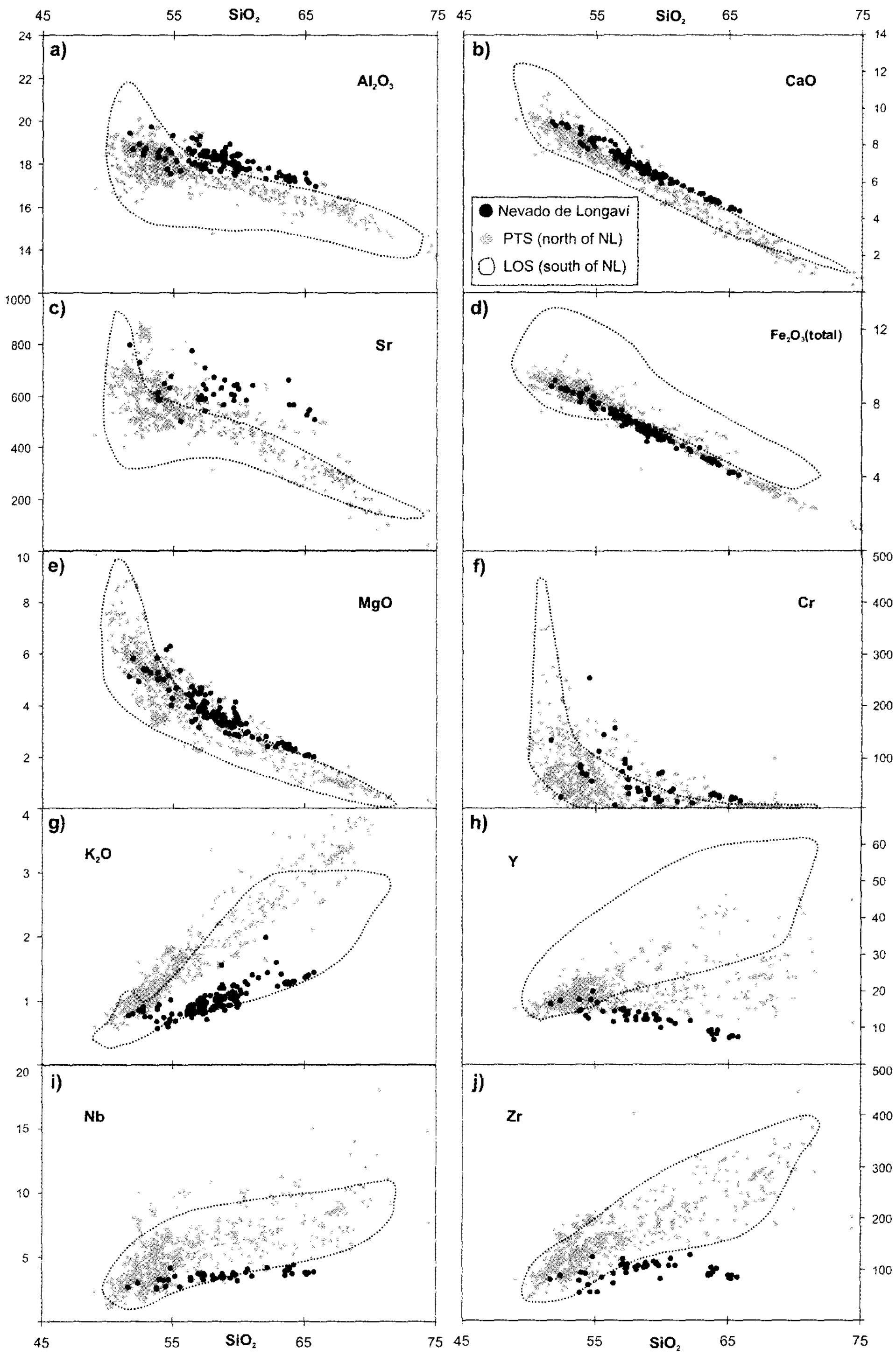

FIG. 7. Major and trace element variations as a function of wt% SiO_2. The data base used as reference includes 383 analyses from the LOS and 910 from the PTS (Fig. 3), 638 of which are from the Tatara-San Pedro complex. Data include literature analyses (various references in text) as well as unpublished data from ongoing projects at the University of Geneva.

The generally low abundances of most incompatible elements in Longaví dacites are further illustrated by normalization of comparable silicic magmas from throughout the SVZ to average SVZ basalt (Fig. 8, Table 1). Longaví dacites are up to an order of magnitude less enriched in highly incompatible elements like Rb and Th, and exhibit HREE depletions comparable to those in volcanoes underlain by putatively thicker crust (TMS). The closest compositional analog to Longaví dacites comes from Mount Burney volcano (52.6°S), which is located in the Austral Volcanic Zone in a considerably different geological and geodynamic context. Adakitic arc magmas from this part of the Andes have been interpreted as oceanic slab melts (Stern and Kilian, 1996). Although we propose a different interpretation for Longaví volcano, it is worth noting that Longaví dacites have the chemical features that characterize 'adakitic' rocks, including (but not limited to) high La/Yb and Sr/Y ratios.

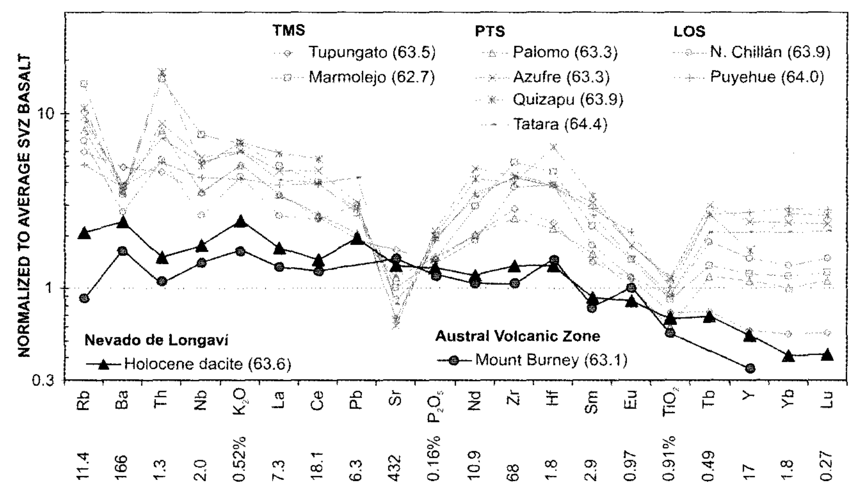

FIG. 8. Nevado de Longaví dacite LLLB01.3 (table 1) compared to rocks with similar SiO_2 contents in the SVZ (numbers in parenthesis are SiO_2 content in an anhydrous basis). All analyses normalized to an average composition of 32 SVZ basalts (<52% SiO_2; normalizing values shown at the base of the diagram). Note that Longaví dacites have lower concentrations of all these elements, except Sr. Note also that a dacite from Mt. Burney (Austral Volcanic Zone) exhibits a similar pattern.

TWO MAGMA SERIES AT NEVADO DE LONGAVÍ

The aggregate Longaví data set displays broad, poorly correlated variations in a number of chemical parameters that can be resolved into two series, here referred to as the low- and high-Rb series (Fig. 9). The chemical signature that renders Longaví volcano unusual is most clearly manifested in the low-Rb series, whereas high-Rb magmas are closer to typical magmas at other nearby centers. The low-Rb series is represented by Holocene dacites and andesites, as well as their quenched mafic enclaves, but it also appears in some of the andesitic flows of the main cone. The high-Rb series is more prevalent in basaltic to andesitic lavas from the early units, some cone-forming andesites, and most of their quenched enclaves. The dominant long-term trend at Nevado de Longaví, thus, is a shift from high- to low-Rb magmas. The timing of this transition, however, is unknown, and the degree to which both series coexisted or alternated remains uncertain, but there is some evidence of mixing between the two series in cone-forming andesitic lavas.

The low-Rb series is characterized by systematically lower concentrations of Th, K_2O, Zr and HREE, and less markedly low Nb, Pb, P_2O_5 and LREE contents (Fig. 10). Moreover, low-Rb magmas of basaltic andesitic composition (53-56 wt% SiO_2) have Rb, Th and Zr concentrations below the average content of SVZ basalts (<52 wt% SiO_2). As the most mafic low-Rb magmas do not represent primitive magmas (low MgO, Cr), this observation is

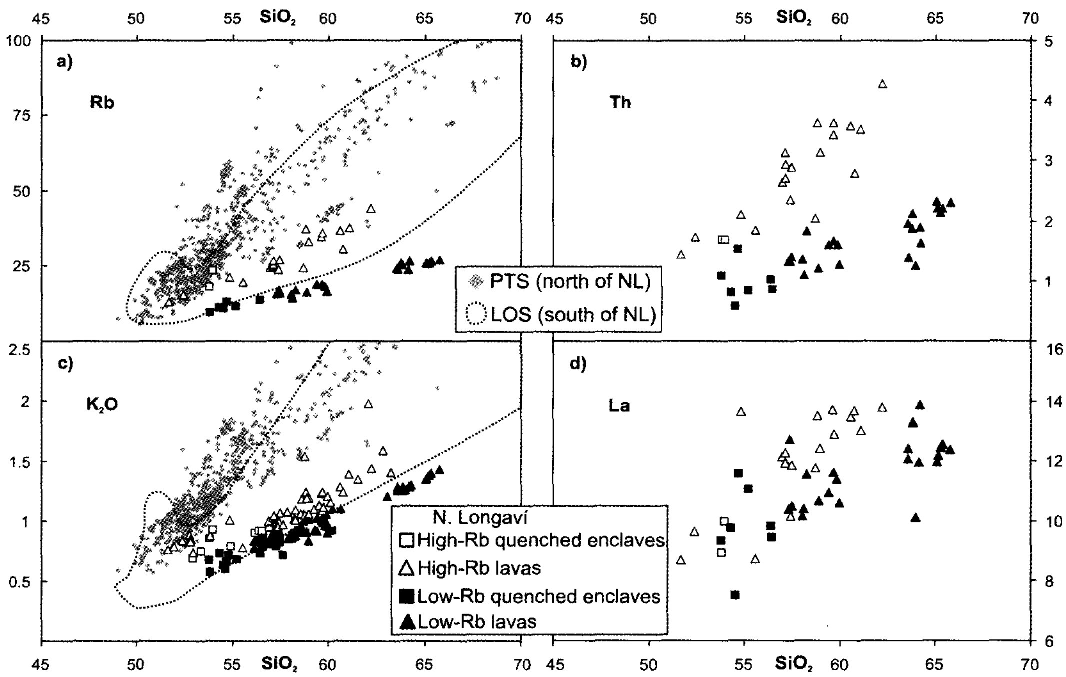

FIG. 9. Distinction between the low-Rb and high-Rb series at Nevado de Longaví volcano. This distinction is particularly clear for Rb *versus* silica (a), but the two groups are also clearly distinguished on the basis of Th (b) and K_2O (c) , and less clearly for La; (d) Note that the low-Rb series diverges from the SVZ data field (a-c).

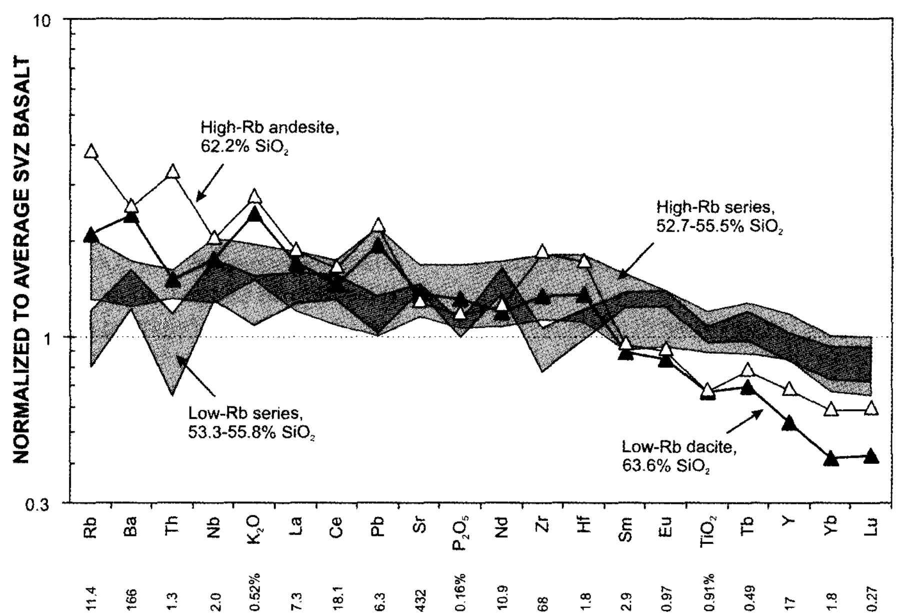

FIG. 10. Comparisons of high-Rb and low-Rb magmas (normalization as in Fig. 8). Individual analyses of evolved magmas are shown by triangles and lines, whereas shaded areas enclose bulk composition of basaltic andesitic magmas. Note that both evolved and mafic low-Rb magmas have noticeably lower abundances of Rb, Th, K_2O, Zr, and HREE despite their slightly higher silica content.

TABLE 1. MAJOR AND TRACE ELEMENT ANALYSES FOR SELECTED NEVADO DE LONGAVÍ SAMPLES. MAJOR ELEMENTS WERE DETERMINED BY X-RAY FLUORESCENCE AT THE UNIVERSITY OF LAUSANNE, SWITZERLAND. VALUES ARE NORMALIZED TO 100% ANHYDROUS BASIS BUT ANALYTICAL TOTAL (1) IS SHOWN. TRACE ELEMENT DATA WERE OBTAINED BY ICP-MS AT HARVARD UNIVERSITY, USA, EXCEPT SAMPLES FROM THE EARLY UNITS (2), DETERMINED BY X-RAY FLUORESCENCE AT LAUSANNE. REPRODUCIBILITY RESULT FOR DUPLICATE ANALYSIS IS BETTER THAN 5% FOR ALL ELEMENTS.

Series	Low-Rb series								High-Rb series												
Unit	Main cone		Holocene						Early units (2)			Main cone					Holocene(?)		Xenoliths		
Sample type	Lava		Pumice		enclave		Dacitic clast (block and ash deposit)		Lava			enclave		Lava			Lava		hbl gabbro	hbl-opx norite	px-hbl gabbronorite
Sample code	NL009	NL028A	Pomez01	Pomez02	LLLINC.3A	MDCP01.1	LLLB01.3	MADHST-2	NL110	NL073	NL078	NL050B	NL050D	NL049	LLG01.4	LMG01.8	NL013	NL014	NL033B	NL015B	NL027B
SiO_2	58,11	59,84	65,78	65,13	53,83	54,32	63,59	64,21	51,94	52,75	53,85	53,83	53,99	57,13	58,96	62,22	51,65	52,40	50,26	51,00	52,63
TiO_2	0,82	0,73	0,52	0,53	0,97	1,02	0,60	0,57	1,03	1,05	1,02	1,05	1,07	0,82	0,79	0,62	1,07	1,09	0,99	1,10	0,94
Al_2O_3	18,53	18,39	16,95	17,28	18,27	18,21	17,38	17,33	18,65	18,43	18,33	18,55	18,61	17,82	18,10	17,81	19,43	18,90	19,94	20,57	19,32
Fe_2O_3(t)	6,57	6,18	4,09	4,22	8,33	8,74	4,91	4,67	9,24	8,81	8,53	8,43	8,53	7,07	6,53	5,38	8,91	8,81	9,46	7,51	8,77
MnO	0,11	0,11	0,08	0,08	0,13	0,13	0,09	0,09	0,14	0,13	0,14	0,13	0,14	0,12	0,11	0,10	0,14	0,14	0,15	0,12	0,14
MgO	3,53	2,86	2,00	2,03	5,27	4,97	2,37	2,23	5,82	5,41	5,03	5,25	5,01	4,63	3,40	2,42	5,13	4,93	5,39	5,59	5,17
CaO	6,80	6,17	4,39	4,58	8,99	7,79	5,13	4,92	9,05	9,13	8,58	8,12	7,96	7,32	6,63	5,54	9,27	9,22	9,60	10,20	8,81
Na_2O	4,43	4,49	4,61	4,62	3,49	3,84	4,46	4,52	3,16	3,20	3,44	3,59	3,53	3,85	4,10	4,28	3,45	3,47	3,75	3,49	3,82
K_2O	0,86	1,00	1,43	1,36	0,57	0,73	1,28	1,28	0,79	0,89	0,88	0,85	0,93	1,03	1,19	1,44	0,76	0,84	0,24	0,33	0,27
P_2O_5	0,23	0,23	0,16	0,17	0,16	0,24	0,18	0,18	0,19	0,20	0,21	0,19	0,22	0,21	0,20	0,19	0,20	0,21	0,20	0,08	0,14
Total (1)	99,97	100,36	100,20	100,03	99,47	99,12	99,96	99,57	99,19	99,27	98,89	100,16	99,98	100,64	99,56	99,83	99,82	100,27	99,65	99,68	100,07
Nb	3,2	3,6	3,8	3,8	2,6	3,1	3,9	4,4	2,5	2,7	3,1	2,6	3,3	3,7	3,4	4,1	2,6	2,9	2,7	2,7	2,5
Zr	98	107	84	83	53	90	88	100	112	118	126	77	93	109	106	126	79	87	21	25	46
Y	12	12	8	8	17	13	9	9	16	15	15	14	15	15	12	12	16	17	13	17	9
Rb	14,4	18,2	26,9	25,5	9,2	11,0	23,6	26,5	10,6	13,8	13,7	18,0	23,2	26,5	33,1	44,0	12,9	15,1	2,7	4,2	3,7
Sr	671	644	509	523	611	646	592	581	761	744	714	588	582	586	602	564	797	730	745	747	788
Ba	294	338	454	449	201	235	433	442	238	249	264	259	271	318	344	428	184	206	168	183	162
Sc	13	12	8	8	30	17	10	9	n.d.	n.d.	n.d.	20	20	17	15	12	21	23	19	29	20
Cr	34	17	18	24	80	67	30	26	88	82	70	86	71	97	28	13	134	24	37	44	42
Ni	28	16	18	18	29	31	19	19	52	56	39	47	43	50	23	14	35	23	30	48	34
La	10,4	11,4	12,4	12,2	9,3	9,8	12,1	13,9	9,0	11,0	11,0	8,9	10,0	11,9	12,4	13,8	8,7	9,7	8,4	7,8	6,8
Ce	22,6	26,3	25,4	25,4	23,8	23,0	27,8	32,0	18,0	20,0	21,0	20,9	23,2	25,9	26,5	30,3	20,9	22,6	22,1	19,7	16,7
Nd	14,0	15,2	12,2	12,3	14,9	14,6	13,4	15,5	n.d.	n.d.	n.d.	13,3	15,1	15,4	13,4	13,7	14,3	14,9	15,3	15,3	11,3
Sm	2,91	3,26	2,22	2,25	3,52	3,32	2,57	2,92	n.d.	n.d.	n.d.	2,95	3,50	3,32	2,96	2,73	3,29	3,50	3,41	3,77	2,23
Eu	0,99	1,03	0,75	0,77	1,32	1,14	0,85	0,93	n.d.	n.d.	n.d.	1,08	1,15	1,10	0,99	0,89	1,10	1,15	1,22	1,29	0,93
Gd	2,81	2,85	1,96	1,95	3,23	3,22	2,24	2,49	n.d.	n.d.	n.d.	3,14	3,55	3,30	2,97	2,66	3,43	3,47	3,23	3,86	2,14
Tb	0,40	0,42	0,30	0,29	0,51	0,45	0,32	0,35	n.d.	n.d.	n.d.	0,48	0,49	0,47	0,42	0,39	0,51	0,54	0,45	0,58	0,32
Yb	1,03	1,10	0,61	0,62	1,65	1,11	0,78	0,86	n.d.	n.d.	n.d.	1,20	1,26	1,39	1,02	1,06	1,48	1,51	1,23	1,43	0,80
Lu	0,15	0,17	0,09	0,09	0,25	0,17	0,12	0,13	n.d.	n.d.	n.d.	0,18	0,18	0,20	0,15	0,16	0,22	0,23	0,17	0,20	0,12
Hf	2,41	2,85	2,23	2,17	1,74	2,41	2,44	2,79	n.d.	n.d.	n.d.	1,96	2,20	2,66	2,69	3,07	2,06	2,38	0,87	1,03	1,34
Pb	9,3	13,0	16,1	13,8	7,4	8,3	10,3	11,6	10,0	11,0	11,0	14,0	6,4	10,6	11,2	14,3	7,2	6,5	5,9	6,1	6,0
Th	1,09	1,60	2,31	2,21	1,08	0,80	1,38	1,64	5,00	6,00	5,00	1,69	1,69	2,94	3,14	4,28	1,43	1,73	0,64	0,50	0,64
U	n.d.	0,4	0,6	0,5	0,3	0,2	0,5	0,6	n.d.	n.d.	n.d.	n.d.	n.d.	n.d.	n.d.	n.d.	n.d.	0,5	n.d.	n.d.	n.d.

consistent with parental magmas that also had low concentrations of these elements. Similarly, greater enrichments of fluid-mobile elements relative to less fluid-mobile elements in the low-Rb series (*e.g.,* high Ba/Th, Pb/Th, Pb/Zr, and Ba/La; Fig. 11a-b) could be inherited from more primitive magmas. Conversely, ratios of elements of similar fluid mobility (Zr/Nb, Zr/La, La/Nb, and Ba/Pb; Fig. 11c-d) show similar values in both series and are comparable to values reported for other volcanic centers. Both series also share a sharp increase in Sr/Y and La/Yb ratios with increasing silica, and at evolved compositions show values that are significantly higher than other SVZ volcanoes despite the fact that mafic magmas are comparable (Fig. 11e-f). The above suggests that the differences between the two series (and between Nevado de Longaví and the rest of the SVZ) are a consequence of both inheritance from distinct parental magmas and of magmatic evolution.

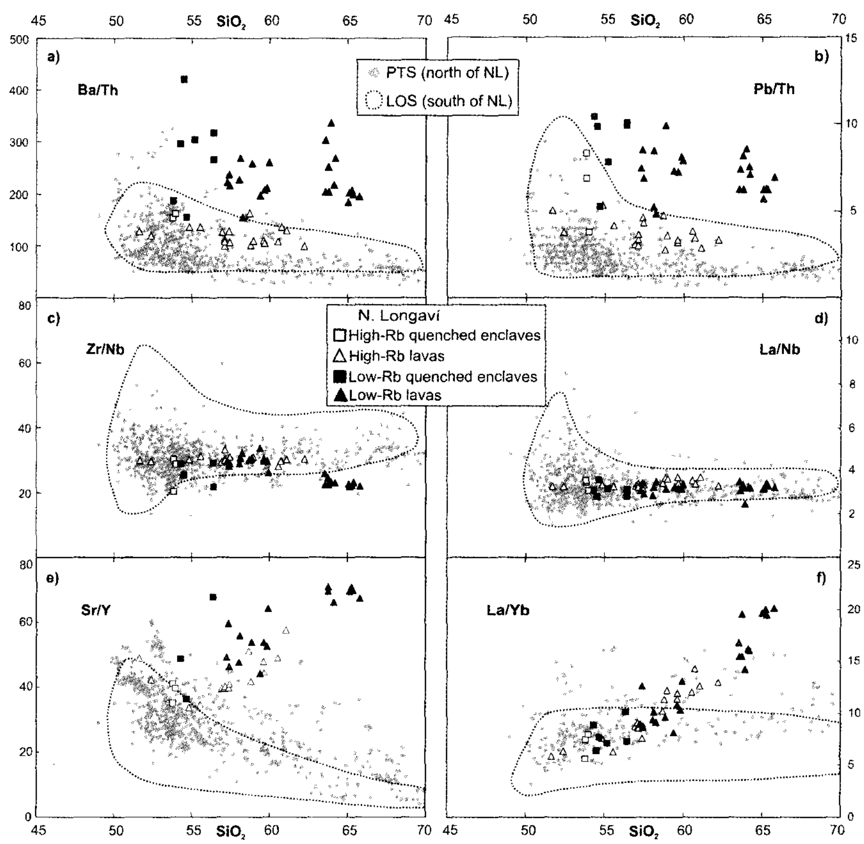

FIG. 11. Trace element ratios versus silica content for Nevado de Longaví magmatic series compared to PTS and LOS segments. Note that in (a) and (b) only low-Rb magmas fall outside the range of values of LOS+PTS; in (c) and (d) both series are within the range, and in (e) and (f) both series diverge from reference values.

MINERAL CHEMISTRY: AMPHIBOLE COMPOSITION AND OXYGEN FUGACITY

High modal amphibole proportions in Longaví magmas are the most obvious mineralogical difference with respect to other SVZ volcanic centers. Amphibole is the dominant mafic phase in quenched mafic enclaves (up to 30 vol%) and in dacites (7-10 vol%), and it is commonly present in andesites of both magma series. In neighboring centers amphibole first appears in rocks with >60 wt% SiO_2

and it is never as abundant as it is at Nevado de Longaví. Amphibole phenocrysts in high-Rb andesites commonly show disequilibrium textures in which amphibole is reacted to fine-grained aggregates of plag+px+opaques (Fig. 6b-c-d). Microprobe analyses of amphiboles from a wide range of whole-rock compositions at Nevado de Longaví are presented in Figure 12, including core analyses from reacted phenocrysts. Important things to notice from these diagrams are: 1) the general distribution into high-Al/Si and low-Al/Si population, plus a less well defined group of transitional character, 2) the nearly identical compositions of amphiboles from low- and high-Rb series andesites, as well as the gabbroic enclaves, and 3) the bimodal distribution of amphiboles from Holocene dacites, in which low-Al/Si amphibole compositions correspond to rims of phenocrysts and cores are high-Al/Si. Amphibole crystals from gabbroic enclaves have compositions that completely overlap those from the lavas, which suggests that gabbroic enclaves are cumulates fractionated from evolving batches of magmas.

Temperature and fO_2 conditions for the magmas have been estimated from microprobe analyses of magnetite-ilmenite pairs. Coexisting grains were analyzed in two dacitic samples and a low-Rb quenched mafic enclave, in addition to two andesites

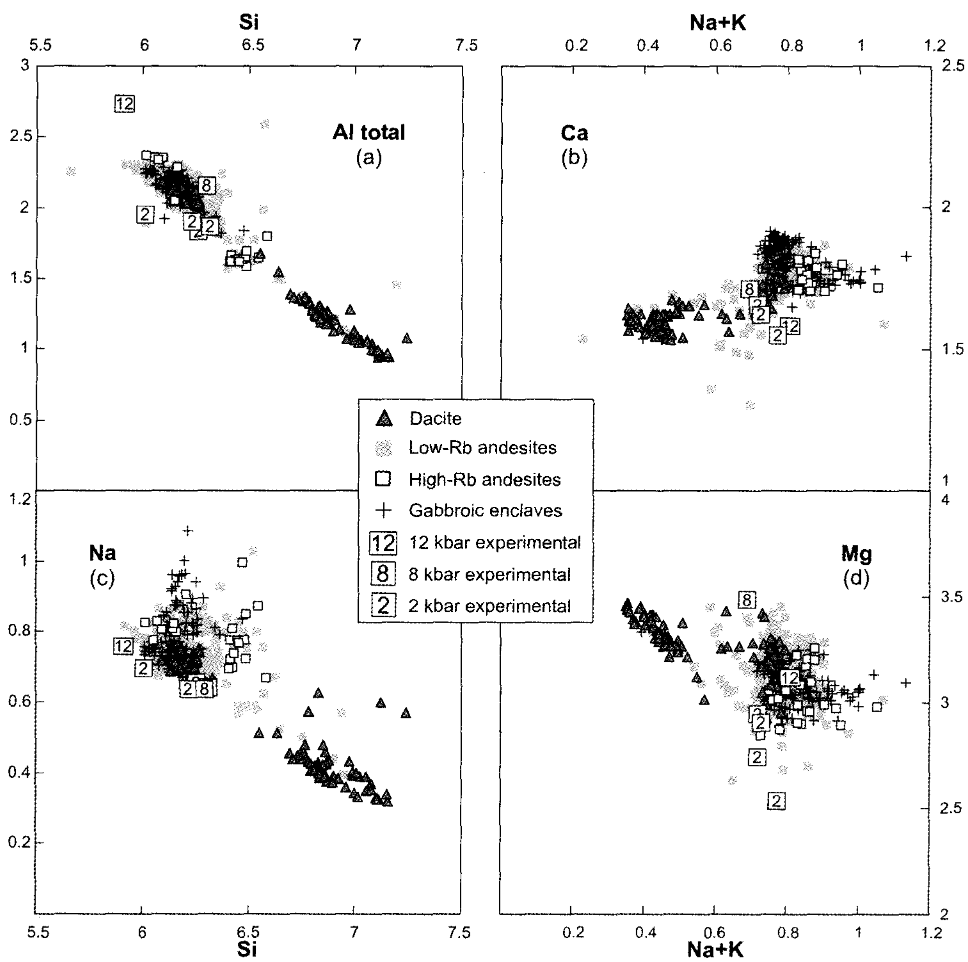

FIG. 12. Chemical compositions of amphiboles in lavas, pyroclastic units and gabbroic enclaves from Nevado de Longaví. Values are in cations per formula unit calculated on a 13-cation basis. Also included for comparison are the chemical compositions of amphiboles crystallized in experiments (12 kbar experiment from Müntener *et al.*, 2001; 8 kbar experiment from Grove *et al.*, 2003; 2 kbar experiments from Grove *et al.*, 1997 and Grove *et al.*, 2003).

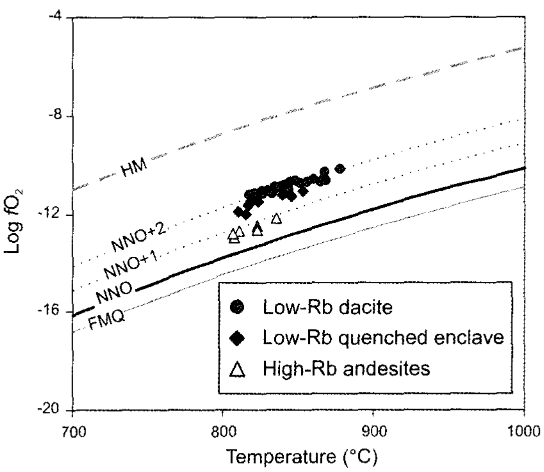

FIG. 13. Temperature versus oxygen fugacity data from magnetite-ilmenite pairs calculated on the basis of the Andersen *et al.* (1993) algorithm. Oxygen fugacity buffers are FMQ= fayalite-magnetite-quartz; NNO= nickel-nickel oxide; HM= hematite-magnetite.

from the high-Rb series. Temperature and fO_2 (Fig. 13) were obtained by the algorithms of Andersen *et al.* (1993) using QUILF95 software for oxide pairs that satisfy the empirical Mg/Mn partitioning test of Bacon and Hischmann (1988). The dacitic samples record the highest fO_2 (NNO+2) and extend to high temperatures around 880°C. These temperatures, however, might need a temperature correction of -30°C whenever high oxygen fugacities are involved (Rutherford and Devine, 1996). Oxide grains in the quenched enclaves record slightly lower temperatures and less oxidizing conditions than the dacite, and probably represent post-mingling conditions because of the late appearance of these phases. The two high-Rb andesite samples record less oxidizing conditions (<NNO+1) than the low-Rb magmas. Although data are still limited, oxidation state may well be another important difference between the two series.

DISCUSSION

Amphibole is commonly present in andesites throughout the volcano, but is especially abundant in the low-Rb series (54-65 wt% SiO_2). Amphibole is, moreover, the dominant mafic phase in the Holocene dacites and mafic enclaves, wherein clinopyroxene is nearly absent. Amphibole crystallization requires high H_2O contents in host magmas (*e.g.,* Rutherford and Devine, 1988), and amphibole proportions can correlate with water contents (*e.g.,* Müntener *et al.*, 2001). Calcic plagioclase (An_{80-90}) crystallized in part simultaneously with amphibole as is recorded in gabbroic cumulates; low-pressure, less calcic plagioclase, however, was probably not largely removed from the magma as is indicated by the positive Al_2O_3 and Sr anomalies in Longaví dacites. Suppression of early plagioclase crystallization and a shift towards more calcic compositions is indicative of high water contents (Sisson and Grove, 1993; Grove *et al.*, 1997), and high mobile-to-immobile element ratios (Ba/Th, Pb/Th) in the low-Rb series is consistent with the water being derived from the subducting slab.

Accumulation of amphibole in enclaves thought to be residual cumulates suggests that, unlike elsewhere in the SVZ, amphibole may be playing a major role in the evolution of Longaví magmas. Amphibole phenocryst cores have SiO_2 contents of 41 to 44 wt%, much lower that the silica contents of clinopyroxene (47-53 wt%) or orthopyroxene (50-55 wt%), thus amphibole fractionation has a higher potential to raise the silica content of the remaining liquid than pyroxene-dominated assemblages. This further implies that liquids derived by fractionation of amphibole-rich assemblages would have a less pronounced increase in the abundance of incompatible elements than liquids derived by fractionation of an anhydrous assemblage.

Large compositional changes in residual liquids due to amphibole crystallization have been documented at Medicine Lake volcano, where the compositional gap between andesites and rhyolites (62-72 wt% SiO_2) was modeled by fractionation of amphibole-rich (17 wt%) assemblages (Grove and Donnelly-Nolan, 1986). What distinguishes Nevado de Longaví is that the proportion of fractionating amphibole might be substantially higher and that this phase starts crystallizing at much less evolved compositions. We have performed a simple mass balance test to calculate the major oxide compositions of residual magmas derived by fractionation of amphibole and An_{85} plagioclase, using the average compositions of the minerals from gabbroic enclaves. Taking a quenched mafic enclave (53.8 wt% SiO_2) as the parental composition, 50% fractionation of 50% amph, 37% plag, 3% cpx, 7% opx, and 3% magnetite is able to produce a residual liquid with 63 wt% SiO_2 and a major element composition similar to Longaví dacites. If incompatible elements are enriched in the residual melt following the Rayleigh fractional crystallization equation $C_l/C_0=F^{D-1}$ (where F is the fraction of remaining liquid and D is the bulk partition coefficient), then a perfectly incompatible element (D=0) will be concentrated in the liquid by a factor of 1/F relative to the original concentration. Removal of 50% of an amphibole-rich assemblage implies that elements with bulk D~0 will be enriched by a maximum factor of 2 (F=0.5), which is in good agreement with the observed enrichments for highly incompatible elements such as Rb, Th, U, Zr, and Nb (*e.g.,* Fig. 10). As a comparison, low-pressure fractionating assemblages such as those proposed for Villarrica volcano and the Planchón-Peteroa complex (Hickey-Vargas *et al.*, 1989; Tormey *et al.*, 1995), involving greater amounts of plagioclase, and pyroxenes and no amphibole, requires 65 to 75% fractionation to achieve the same silica increase, and incompatible elements would be enriched by factors of 3 to 4.

Crystallization of amphibole from relatively mafic magmas has been documented experimentally wherein starting materials are water-rich (up to water saturated) basalts and basaltic andesites (*e.g.,* Grove *et al.*, 1997; Moore and Carmichael, 1998; Müntener *et al.*, 2001; Grove *et al.*, 2003), with a wide range of pressures from 2 to 20 kbar and fO_2 between NNO and NNO+4. Amphibole has crystallized in high proportions in experiments wherein starting materials are hydrated arc basalts. For example, at 8 kbar and with a water-saturated high-Mg basalt as starting material, modal amphibole is 60 vol% only 25°C below the liquidus temperature, in equilibrium with basaltic andesitic glass (run 373; Grove *et al.*, 2003). At the same pressure, plagioclase is also inferred to join at lower temperatures. In higher pressure experiments (12 kbar), Müntener *et al.* (2001) obtained trace amounts of garnet (0.1%) in addition to amphibole and pyroxene from a basaltic starting material with ~5 wt% H_2O added.

Fractionation of a hornblende-rich assemblage from very hydrous magmas may thus account for some of the chemical characteristics of intermediate to evolved compositions, but it does not explain the low incompatible element abundances observed in the most mafic quenched magmatic enclaves and in their inferred parental magmas. Fluid-mobile elements such as Ba and Pb are interpreted in arc settings to be mostly supplied by fluids derived from dehydration of the subducted slab and/or sediments, whereas the concentration of less soluble elements like Th, Nb, and Zr will be largely controlled by their concentrations in the mantle source and the degree of melting (*e.g.,* Davidson, 1996). Relative enrichments of fluid-mobile elements in the low-Rb series (higher Ba/Th, Ba/La, Pb/Th, and Rb/Zr ratios than in the high-Rb series), may reflect that the proportion of slab-derived fluids involved in the genesis of low-Rb parental magmas is higher than in those parental to high-Rb magmas. In contrast, similar Zr/Nb, Zr/La, and La/Nb ratios in both series argue in favor of a similar mantle source for both magma types. An expected consequence of enhanced water supply to the mantle source region is higher degrees of melting (Hickey-Vargas *et al.*, 1989; Asimow and Langmuir, 2003; Katz *et al.*, 2003), and hence, the resulting primitive liquids will be less enriched in non-fluid mobile incompatible elements than lower degree melts from the same source. If high-degree wet melts are parental to low-Rb quenched mafic enclaves, important olivine +pyroxene fractionation must be invoked in order to explain the relatively low concentrations of Mg, Ca and Sc observed in these enclaves. High-pressure olivine and pyroxene fractionation is the main mechanism inferred for the generation of SVZ basalts from primitive mantle-derived melts.

La/Yb and Sr/Y increases with increasing silica in both series are due to a decrease in concentrations of HREE and Y by a factor of ~0.5 within the range of 53 to 63 wt% SiO_2. If crystal fractionation is responsible for these depletions, bulk partition coefficients for HREE and Y must be in the neighborhood of 2 to 2.3. Assuming that amphibole constitutes 50% of the fractionating assemblage and F=0.5, in concert with the major element model, amphibole/liquid partition coefficients for Y and Yb should be around 4 and 4.3 respectively to account for the observed variations. Measured amphibole/melt partition coefficients for Y and Yb in calcalkaline magmas are within the range of 1.0-2.1 (*e.g.,* Bacon and Druitt, 1988; Sisson 1994; Brenan *et al.*, 1995; Klein *et al.*, 1997), although at high pressures (12 kbar) and relatively low temperatures (~980°C) coefficients up to 3.4 for Y have been measured (Blundy, *oral communication*). It seems likely, therefore, that high La/Yb related to decreasing HREE in Longaví volcano magmas is in part due to garnet fractionation. Increasing La/Yb and Sr/Y are also observed in the high-Rb series, where amphibole appears to be a less abundant fractionating phase. An important corollary to this observation is that most of the evolution of Longaví magmas may have occurred at depths where garnet is stable in hydrous calcalkaline magmas (>~8 kbar; Ulmer *et al.*, 2003), and that little differentiation is taking place at the upper crustal levels.

ARE OCEANIC FRACTURES PLAYING A ROLE?

There are good reasons to suspect that the asthenospheric mantle below Longaví volcano may be supplied with unusual amounts of water. The horizontal projection of the Mocha Fracture Zone beneath the continent intersects the volcanic front in the vicinity of Longaví volcano. Oceanic fractures are a potentially very efficient means for transporting water into the asthenospheric mantle because they commonly host serpentinitic bodies deep into the oceanic lithosphere. Fully serpentinized oceanic lithosphere can contain up to 11-13 wt% H_2O, *i.e.*, it is an order of magnitude more efficient in liberating H_2O at depth than hydrous minerals from altered oceanic crust (Ulmer and Trommsdorff, 1995). Singer *et al.* (1996) proposed that in the Aleutian arc the Amlia fracture zone acts as a transport of fluids and trench sediments into the subarc mantle, and that as a consequence, overlying volcanoes erupt lavas derived from high melting degrees and with high fluid-mobile element concentrations.

Oceanic fracture zones are currently being subducted at other points along the arc, and are likely to be exerting a similar role to what is inferred to be happening at Longaví volcano (Fig. 1). It is possible that the evolved products from the Mocho-Choshuenco complex and Calbuco volcano, located over the projections of the Valdivia and Chiloé fracture zones respectively, constitute somewhat similar cases to Longaví volcano. Both of these centers have erupted evolved rocks that contain amphibole and in which the behavior of incompatible element abundances and ratios is also similar to what is observed at Longaví volcano (Fig. 14), although crustal contamination has been identified for magmas from both of these centers (McMillan *et al.*, 1989: López-Escobar *et al.*, 1992; Hickey-Vargas *et al.*, 1995). The incompatible element-poor nature of the andesites from Calbuco volcano has been suggested by López-Escobar *et al.* (1995b) to be a consequence of fractionation of hornblende-rich assemblages. They propose that the water needed to stabilize amphibole in the system is derived from the assimilation of hydrous, metasedimentary crust, which is in agreement with the relatively high Sr isotope ratios observed, but is contradicted by the low abundances of incompatible elements that characterize the volcanic suite. The fact that these volcanoes do not show significant Y depletions (and hence, low Sr/Y ratios) might be related to differences in crustal thickness, where garnet stability is not attained further south.

SUMMARY AND CONCLUSIONS

Nevado de Longaví magmas show a number of mineralogical and chemical features that make them distinctive from other SVZ magmas. Elevated water supply to the mantle source region is consistent with most first-order features that characterize Longaví magmas. The recognition of two magmatic series present at Longaví volcano suggests that magma generation conditions have not been stable through time, although the timing of transition from one series to the next is unconstrained. The low incompatible element abundances that characterize Longaví evolved magmas, and especially the low-Rb series, is probably the result of fractionation of low-SiO_2 amphibole in much higher proportions than in other SVZ centers. Genesis of low-Rb mafic magmas is explained in terms of high degrees of melting of a mantle source in response to high fluid inputs coming from the slab. High-Rb andesitic magmas are less markedly distinct from other SVZ magmas, and may have evolved from less hydrous primitive melts. The authors propose that the oceanic Mocha Fracture Zones is responsible for the high water supply to the subarc mantle beneath Nevado de Longaví, and that oceanic fractures subducted further south could be influencing in a similar way the composition of magmas from other volcanoes in the SVZ.

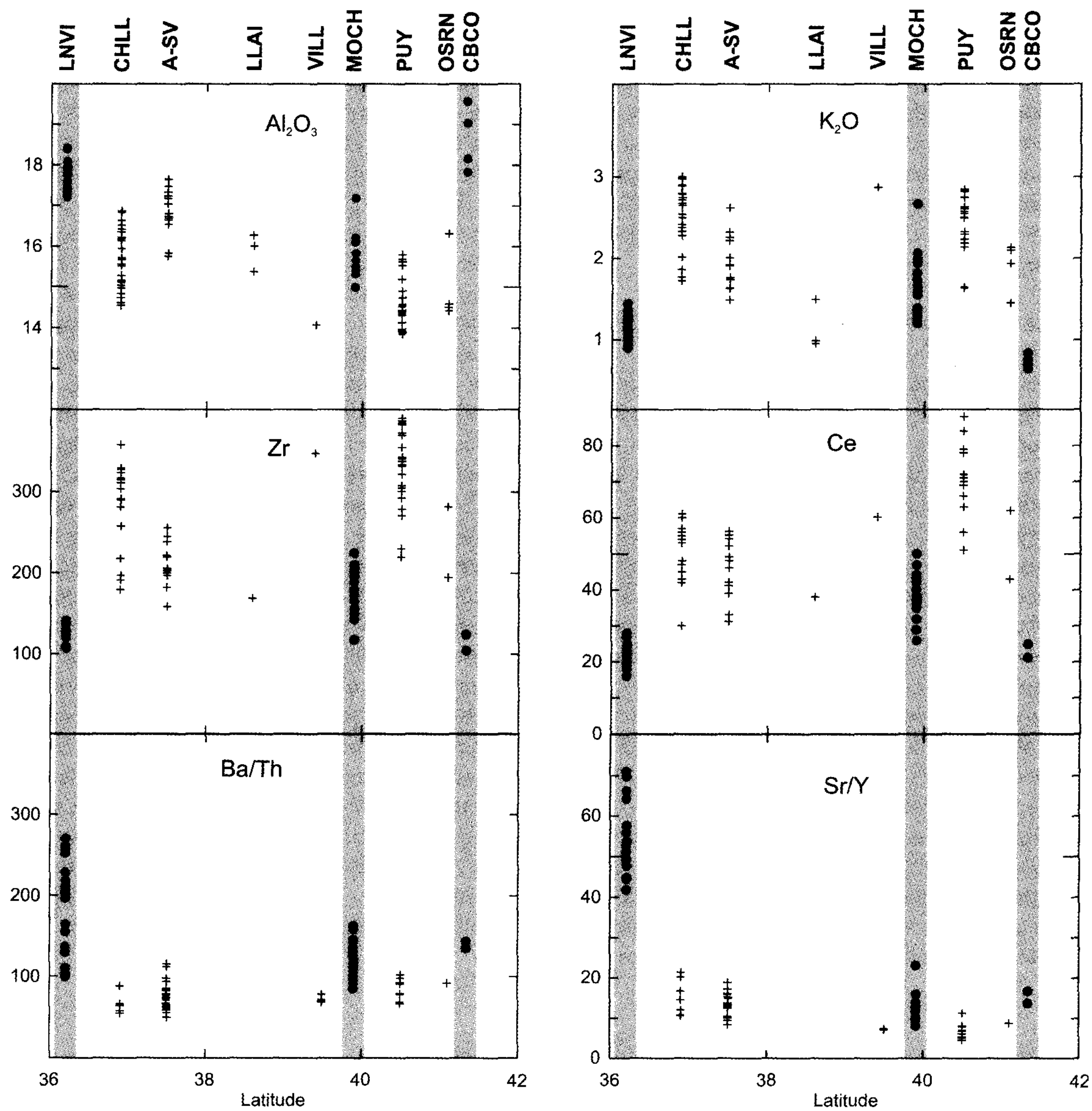

FIG. 14. Compositions of rocks with 58%<SiO_2<65% versus latitude for centers south of Longaví volcano. LNVI: Nevado de Longaví, CHLL: Nevados de Chillán, A-SV: Antuco-Sierra Velluda, LLAI: Llaima, VILL: Villarica, MOCH: Mocho-Choshuenco, PUY: Puyehue, OSRN: Osorno, CBCO: Calbuco. Highlighted volcanoes correspond to those located over oceanic fracture zones (see Fig. 1).

ACKNOWLEDGEMENTS

Work for this project is financed by the Swiss Fonds National grant #2000-063950.00. D.S. benefited in 2001-2003 from a fellowship from the Swiss Confederation. S. Kay, W. Hildreth, and L. López-Escobar are sincerely acknowledged for constructive reviews that greatly helped improve the paper. We thank SERNAGEOMIN for logistical support provided during field work. F. Costa, G. Morris, A. Marzoli and R. Spikings made helpful revisions of early versions of the manuscript.

REFERENCES

Andersen, D.; Lindsley, D.; Davidson, P. 1993. QUILF: a pascal program to assess equilibria among the Fe-Mg-Mn-Ti oxides, pyroxenes, olivine, and quartz. *Computers and Geosciences,* Vol. 19, p. 1333-1350.

Asimow, P.D.; Langmuir, C.H. 2003. The importance of water to oceanic mantle melting regimes. *Nature,* Vol. 421, p. 815-820.

Bacon, C.R.; Druitt, T.H. 1988. Compositional evolution of the zoned calc-alkaline magma chamber of Mt. Mazama, Crater Lake, Oregon. *Journal Contributions to Mineralogy and Petrology,* Vol. 98, p. 224-256.

Bacon, C.; Hirschmann, M. 1988. Mg/Mn partitioning as a test for equilibrium between coexisting Fe-Ti oxides. *American Mineralogist,* Vol. 73, p. 57-61.

Bohm, M.; Lüth, S.; Echtler, H.; Asch, G.; Bataille, K.; Bruhn, C.; Rietbrock, A.; Wigger, P. 2002. The Southern Andes between 36° and 40°S latitude: seismicity and average seismic velocities. *Tectonophysics,* Vol. 356, p. 275-289.

Brenan, J.M.; Shaw, H.F.; Ryerson, F.J.; Phinney, D.L. 1995. Experimental determination of trace element partitioning between pargasite and a synthetic hydrous andesitic melt. *Earth and Planetary Science Letters,* Vol. 135, p. 1-11.

Davidson, J.P. 1996. Deciphering mantle and crustal signatures in subduction zone magmatism. *In* Subduction from Top to Bottom (Bebout, G.; Kirby, S.; Scholl, D.; Platt, J.; editors). American *Geophysical Union Monograph,* No. 96, p. 251-262. Washington, D.C.

Davidson, J.P.; Dungan, M.A.; Ferguson, K.M.; Colucci, M.T. 1987. Crust-magma interactions and the evolution of arc magamas; the San Pedro-Pellado volcanic complex, southern Chilean Andes. *Geology,* Vol. 15, p. 443-446.

Dungan. M.A.; Wulff, A.; Thompson, R. 2001. Eruptive stratigraphy of the Tatara-San Pedro complex, 36°S, Southern Volcanic Zone, Chilean Andes: Reconstruction method and implications for magma evolution at long-lived arc volcanic centers. *Journal of Petrology,* Vol. 42, No. 3, p. 555-626.

Feeley, T.C.; Dungan, M.A. 1996. Compositional and dynamic controls on mafic-silicic magma interactions at continental arc volcanoes: evidence from Cordón El Guadal, Tatara-San Pedro Complex, Chile. *Journal of Petrology,* Vol. 37, No. 6, p. 1547-1577.

Futa, K.; Stern, C. 1988. Sr and Nd isotopic and trace element compositions of Quaternary volcanic centers of the southern Andes. *Earth and Planetary Science Letters,* Vol. 88, p. 253-262.

Gardeweg, M. 1980. Geología del área del Nevado de Longaví, Cordillera de los Andes, VII Región del Maule. Memoria de Título (Unpublished), *Universidad de Chile, Departamento de Geología,* 247 p.

Gardeweg, M. 1981. El volcanismo Cenozoico Superior del área del Nevado de Longaví: una zona de transición en los Andes de Chile central. *In Congreso Geológico Argentino, No. 8, Actas,* Vol. 3, p. 221-240. San Luis, Argentina.

Grove, T.L.; Donnelly-Nolan, J.M. 1986. The evolution of young silicic lavas at Medicine Lake volcano, California: implications for the origin of compositional gaps in calc-alkaline series lavas. *Contributions to Mineralogy and Petrology,* Vol. 92, p. 281-302.

Grove, T.L.; Donnelly-Nolan, J.M.; Housh, T. 1997. Magmatic processes that generated the rhyolite of Glass Mountain, Medicine Lake volcano, N. California. *Contributions to Mineralogy and Petrology,* Vol. 127, p. 205-223.

Grove, T.L.; Elkins-Tanton, L.T.; Parman, S.W.; Chatterjee, N.; Müntener, O.; Gaetani, G.A. 2003. Fractional crystallization and mantle-melting controls on calc-alkaline differentiation trends. *Contributions to Mineralogy and Petrology,* Vol. 145, p. 515-533.

Herron, E.M. 1981. Chile Margin near lat 38°S: Evidence for a genetic relationship between continental and marine geologic features or a case of curious coincidences? *Geological Society of America, Memoir* 154, p. 755-760.

Hickey, R.L.; Gerlach, D.C.; Frey, F.A. 1984. Geochemical variations in volcanic rocks from central-south Chile (33-42°S). *In* Andean magmatism, chemical and isotopic constraints (Harmon, R.S.; Barreiro, B.A.; editors). *Shiva Publishing Ltd.,* p. 72-95. Cheshire.

Hickey-Vargas, R.; Moreno, H.; López, L.; Frey, F.A. 1989. Geochemical variations in Andean basaltic and silicic lavas from the Villarica-Lanin volcanic chain (39.5°S): an evaluation of source heterogeneity, fractional crystallization and crustal assimilation. *Contributions to Mineralogy and Petrology,* Vol. 103, p. 361-386.

Hickey-Vargas, R.; Abdollahi, M.J.; Parada, M.A.; López-Escobar, L.; Frey, F.A. 1995. Crustal xenoliths from Calbuco volcano, Andean Southern Volcanic Zone: implications for crustal composition and magma-crust interaction. *Contributions to Mineralogy and Petrology,* Vol. 119, p. 331-344.

Hildreth, W.; Moobath, S. 1988. Crustal contributions to arc magmatism in the Andes of Central Chile. *Contributions to Mineralogy and Petrology,* Vol. 98, p. 455-489.

Hildreth, W.; Moobath, S. 1991. Reply to Comment on 'Crustal contributions to arc magmatism in the Andes of Central Chile' by W. Hildreth and S. Moorbath. *Contributions to Mineralogy and Petrology,* Vol. 108, p. 247-252.

Katz, R.; Spiegelman, M.; Langmuir, C.H. 2003. A New Parameterization of Hydrous Mantle Melting.

Geochemistry, Geophysics, Geosystems (G^3), electronic journal. Vol. 4, No. 9, 1073 DOI 10.1029/2002GC000433.

Klein, M.; Stosch, H.-G.; Seck, H.A. 1997. Partitioning of high-strength and rare-earth elements between amphibole and quartz-dioritic to tonalitic melts: an experimental study. *Chemical Geology,* Vol. 138, p. 257-271.

Le Maitre, R.W. (editor). 1989. A classification of igneous rocks and glossary of terms. Recommendations of the International Union of Geological Sciences, Subcommission on the Systematics of Igneous Rocks. *Blackwell Scientific Publications,* Oxford, 193 p.

López-Escobar, L. 1984. Petrology and chemistry of volcanic rocks of the southern Andes. *In* Andean magmatism, chemical and isotopic constraints (Harmon, R.S.; Barreiro, B.A.; editors). *Shiva Publishing Ltd.,* p. 47-71.Cheshire.

López-Escobar, L.; Parada, M.A.; Moreno, H.; Frey, F.A.; Hickey-Vargas, R.L. 1992. A contribution to the petrogenesis of Osorno and Calbuco volcanoes, Southern Andes (41°00'-41°30'S): comparative study. *Revista Geológica de Chile,* Vol. 19, No. 2, p. 211-226.

López-Escobar, L.; Kilian, R.; Kempton, P.D.; Tagiri, M. 1993. Petrography and geochemistry of Quaternary rocks from the Southern Volcanic Zone of the Andes between 41°30' and 46°00'S, Chile. *Revista Geológica de Chile,* Vol. 20, No. 1, p.33-55.

López-Escobar, L.; Cembrano, J.; Moreno, H. 1995a. Geochemistry and tectonics of the Chilean Southern Andes basaltic Quaternary volcanism (37-46°S). *Revista Geológica de Chile,* Vol. 22, No. 2, p. 219-234.

López-Escobar, L.; Parada, M.A.; Hickey-Vargas, R.; Frey, F.A.; Kempton, P.D.; Moreno, H. 1995b. Calbuco volcano and minor eruptive centers distributed along the Liquiñe-Ofqui Fault Zone, Chile (41°-42°S): contrasting origins of andesitic and basaltic magma in the Southern Volcanic Zone of the Andes. *Contributions to Mineralogy and Petrology,* Vol. 119, p. 345-361.

McMillan, N.J.; Harmon, R.S.; Moorbath, S.; López-Escobar, L.; Strong, D.F. 1989. Crustal sources involved in continental arc magmatism: a case study of volcán Mocho-Choshuenco, southern Chile. *Geology,* Vol. 17, p. 1152-1156.

Moore, G.; Carmichael, I.S.E. 1998. The hydrous phase equilibria (to 3 kbar) of an andesite and basaltic andesite from western Mexico: constraints on water content and conditions of phenocryst growth. *Contributions to Mineralogy and Petrology,* Vol. 130, p. 304-319.

Muñoz, J. and Niemeyer, C. 1984. Hoja Laguna del Maule, Regiones del Maule y del Bío Bío. *Servicio Nacional de Geología y Minería, Carta Geológica de Chile,* No.64.

Müntener, O.; Kelemen, P.B.; Grove, T.L. 2001. The role of H_2O during crystallization of primitive arc magmas under uppermost mantle conditions and genesis of igneous pyroxenites: an experimental study. *Contributions to Mineralogy and Petrology,* Vol. 141, p. 643-658.

Naranjo, J.A.; Haller, M.J. 2002. Erupciones holocenas principalmente explosivas del volcán Planchón, Andes del sur (35°15'S). *Revista Geológica de Chile,* Vol. 29, No. 1, p. 93-113.

Ruiz, J.; Hildreth, W.; Chesley, J. 2001. Crust-mantle contributions to Andean magmas. *In Simposio Sudamericano de Geología Isotópica, No. 3,* p. 340-341. Pucón.

Rutherford, M.J.; Devine, J.D. 1988. The may 18, 1988 eruption of Mt. St. Helens 3. Stability and chemistry of amphibole in the magma chamber. *Journal of Geophysical Research,* Vol. 93, p. 11949-11959.

Rutherford, M.J.; Devine, J.D. 1996. Preeruption pressure-Temperature conditions and volatiles in the 1991 dacitic magma of Mount Pinatubo, *In* Fire and Mud, eruptions and lahars of Mount Pinatubo, Philippines (Newhall, C.G.; Punongbayan, R.S.; editors*), Philippine Institute of Volcanology and Seismology and University of Washington Press,* p. 751-766, Hong Kong.

Sigmarsson, O.; Condomines, M.; Morris, J.D.; Harmon, R.S. 1990. Uranium and ^{10}Be enrichments by fluids in Andean arc lavas. *Nature,* Vol. 346, p. 163-165.

Singer, B.S.; Leeman, W.; Thirlwall, M.; Rogers, N. 1996. Does Fracture zone subduction increase sediment flux and mantle melting in subduction zones? Trace element evidence from Aleutian arc basalt. *In* Subduction from Top to Bottom. Bebout, G.; Kirby, S.; Scholl, D.; Platt, J.; editors). *American Geophysical Union Monograph* No. 96, p. 285-291. Washington D.C.

Sisson, T.W. 1994. Hornblende-melt trace-element partitioning measured by ion microprobe. *Journal Chemical Geology,* Vol. 117, p. 331-344.

Sisson, T.W.; Grove, T.L. 1993. Experimental investigations of the role of water in calc-alkaline differentiation and subduction zone magmatism. *Contributions to Mineralogy and Petrology,* Vol. 113, p. 143-166.

Stern, C.R. 1991. Comment on 'Crustal contributions to arc magmatism in the Andes of Central Chile' by W. Hildreth and S. Moorbath. *Contributions to Mineralogy and Petrology,* Vol. 108, p. 241-246.

Stern, C.R. 2004. Active Andean Volcanism: its geologic and tectonic setting. *Revista Geológica de Chile,* Vol. 31, No. 2, p. 161-206.

Stern, C.R.; Kilian, R. 1996. Role of the subducted slab, mantle wedge and continental crust in the generation of adakites from the Andean Austral Volcanic Zone. *Contributions to Mineralogy and Petrology,* Vol. 123, p. 263-281.

Tebbens, S.F.; Cande, S.C. 1997. Southeast Pacific tectonic evolution from early Oligocene to Present. *Journal of Geophysical Research,* Vol. 102, p. 12061-12084.

Tormey, D.R.; Hickey-Vargas, R.; Frey, F.A.; López-Escobar, L. 1991. Recent lavas from the Andean volcanic front (33 to 42°S); interpretations of along-arc compositional variations. *In* Andean magmatism and its tectonic setting (Harmon, R.S.; Rapela, C.W.; editors). *Geological Society of America, Special Paper* 265, p. 57-77.

Tormey, D.R.; Frey, F.A.; López-Escobar, L. 1995. Geochemistry of the active Azufre-Planchón-Peteroa volcanic complex, Chile (35°15'S): evidence for multiple sources and processes in a cordilleran arc magmatic system. *Journal of Petrology*, Vol. 36, No. 2, p. 265-298.

Ulmer, P.; Trommsdorff, V. 1995. Serpentinite stability to mantle depths and subduction related magmatism. *Science*, Vol. 268, p. 858-861.

Ulmer, P.; Müntener, O.; Alonso-Pérez, R. 2003. Potential role of garnet fractionation in H_2O-undersaturated andesite liquids at high pressure: an experimental study and a comparison with the Kohistan arc. *Geophysical Research Abstracts*, Vol. 5, 08308, EGS-AGU-EUG Meeting, Nice, France.

Wood, C.A.; Nelson, K.L. 1988. Inter-segment variation of magmatic composition in the Andes of Central Chile. *EOS Transactions, American Geophysical Union*, Vol. 69, p. 1494.

Manuscript received: September 12, 2003; accepted: August 9, 2004.